

# Long-term optical spectroscopy of B[e] star CI Cam in a quiet state

Valentina G. Klochkova,<sup>1,\*</sup> Anatoly S. Miroshnichenko,<sup>2,3</sup> Vladimir E. Panchuk<sup>1</sup>

<sup>1</sup>*Special Astrophysical Observatory, Nizhnij Arkhyz, 369167 Russia*

<sup>2</sup>*University of North Carolina at Greensboro,*

*PO Box 26170, Greensboro, NC 27402-6170, USA*

<sup>3</sup>*Fesenkov Astrophysical Institute, Observatory 23, 050023, Almaty, Kazakhstan*

High-resolution optical spectra of the B[e] star CI Cam were obtained on arbitrary dates 2002–2023 using the echelle spectrograph NES of the 6-m BTA telescope. The temporal variability of the powerful emissions of H $\alpha$  and HeI profiles is found. For two-peaked emissions with “rectangular” profiles, the intensity ratio of blue-shifted and red-shifted peaks is  $V/R \geq 1$ , except one date. A decrease in the intensity of all double-peaked emissions with “rectangular” profiles was revealed as they moved away in time from the 1998 outburst. The average radial velocity for emissions of this type for all observational dates varies in the range  $(-50.8 \div -55.7) \pm 0.2$  km/s. The half-amplitude of the change (standard deviation) is equal to  $\Delta V_r = 2.5$  km/s. The velocity for single-peaked ion emissions (Si III, Al III, Fe III) differs little from the values of  $V_r(\text{emis-d})$ , but the measurement accuracy for these emissions is worse: the average error for different dates ranges from 0.4 to 1.3 km/s. The systemic velocity is assumed to be  $V_{\text{sys}} = -55.4 \pm 0.6$  km/s according to the stable position of the forbidden emission [N II] 5754 Å. The position of single-peaked emissions [O III] 4959 and 5007 Å is also stable:  $V_r(\text{[O III]}) = -54.2 \pm 0.4$  km/s. Forbidden emissions [O I] 5577, 6300, 6363 Å, [Ca II] 7291 and 7324 Å are absent from the spectra. Appearance of the emission near 4686 Å is an infrequent event, its intensity rarely exceeds the noise level. Only a wide asymmetric emission with an intensity of about 16% above the local continuum was registered in the spectrum for March 9, 2015. Questions arise about the use of this emission to estimate the period of variability of the star and about localization of this feature in the CI Cam system. The photospheric absorptions of N II, S II, and Fe III with a variable position are identified.

**Keywords:** *massive stars, binary systems, CI Cam, optical spectra, variability*

## 1. INTRODUCTION

The hot star CI Cam has long been known as a star with an optical spectrum rich in emissions, it is designated MWC 84 in the catalog [1]. Particular interest in this object arose after the registration of a powerful outburst in its system in April 1998, which was observed in all spectral ranges from X-ray to radio [2]. After this event, the star was classified as an ultraluminous X-ray source (for more details, see [3]) and is studied intensively in all wavelength ranges, the SIMBAD database contains over 250 publications. The main features of the optical spectrum of CI Cam intense emissions of HI, HeI, as well as emissions

---

\*Electronic address: [Valentina.R11@yandex.ru](mailto:Valentina.R11@yandex.ru)

of Fe II, [Fe II] with specific “rectangular” profiles, were identified already in early articles [4, 5], whose authors classified the star as a supergiant with the B[e] phenomenon. Let us recall that the first interpretation of emission “rectangular” profiles for stars with constant loss of matter was given by Beals [6], using the example of recorded emission bands with flat tops in the spectra of Wolf–Rayet stars and Novae. By now, there is a widespread idea that emissions in the spectra of stars with the B[e] phenomenon are formed in a structured circumstellar medium in the form of a dense disk and/or arcs. Zickgraph [7] summarized the fundamental features of the optical spectra of B[e] stars and carried out theoretical modeling of the profiles of specific spectral features. The presence of forbidden lines of metals in the optical spectrum caused by their formation within a low-density circumstellar medium close to the star, is considered as the main feature of stars with the B[e] phenomenon.

Just a few days after the 1998 outburst CI Cam spectroscopy in the IR range revealed powerful emissions of HI, He, Fe and their subsequent changes [8]. The results of the first observations in various wavelength ranges stimulated a number of observational campaigns, the results of which were later summarized in numerous original articles and reviews. Let us note the most important publications for understanding the features of the optical spectrum of CI Cam (and related objects): these are [3, 7–9]. Important for understanding the features of stars with the B[e] phenomenon is the work [10]. The authors of this work, having obtained high-resolution spectra for a sample of stars, studied the variability of emissions and came to the conclusion that specific emissions arise in a set of envelopes structures. To study the long-term behavior of the optical spectrum, CI Cam has no analogues with high spectral resolution observations made two weeks after the 1998 outburst at the 2.7-m telescope of the McDonald Observatory, which allowed the authors [11] identify the components of the spectrum in detail, estimate their parameters and indicate the areas of formation of various types of emissions.

Several groups of astronomers have studied the time behavior of photometric and spectral parameters of CI Cam. The principal results were obtained through spectral monitoring carried out by the authors [12], which tracked changes in the profiles of the main emissions in the optical spectrum during 2001–2005, in particular, a transition of the H $\alpha$  profile was recorded from double-peak type to single-peaked type. These authors highlighted the significant error in determining equivalent widths of spectral features due to continuum level uncertainty. An important result—the detection of an inclined dust disk – was obtained by interferometry in the near-infrared range [13]. Goranskij et al. [14], using an extensive collection of spectra obtained with some spectrographs of the 6-m BTA telescope, providing different spectral resolutions, made a number of significant conclusions. In particular, the study of the radial velocity V<sub>r</sub> pattern along lines of various natures (He II 4686 Å, [N II] 5754 Å and Fe II) revealed a special behavior of the forbidden emission [N II] 5754 Å, which allowed the authors to conclude that this line is formed in a region more distant from the star compared to that for the Fe II emissions.

To date, the main ideas about the structure and behavior of CI Cam can be briefly summarized as follows: CI Cam is a B[e] phenomenon object, which includes a massive star of early spectral class B and a low-mass companion of an as yet unknown nature; several years after the 1998 outburst, the type of emissions in the optical spectrum changed and their intensity decreased significantly; the complex structure of the circumstellar medium was formed due to fast polar wind and a slow equatorial outflow; there are no absorption features in the optical spectrum, with the exception of interstellar absorptions; there are no reliable estimates of the distance, luminosity and orbital parameters; for example, there is

no generally accepted value for the orbital period.

The need for numerous high-quality spectral data is obvious, so publications often end with a call for such observations. However, the large distance of the CI Cam (parallax  $\pi=0.21$  mas according to Gaia EDR3 [15]) hinders the regular high-resolution spectral monitoring needed to generate a comprehensive collection of spectra. As M. Kraus correctly noted in her review [9], performing such monitoring requires a lot of patience and a lot of time on large telescopes. So far, only a few studies have been published with results based on the analysis of high-resolution spectra obtained at individual points in time, for example, [3, 5]. In an effort to increase time observations interval, the authors are forced to combine measurement data obtained from observations with high and low spectral resolution [14].

The lack of observational data of the required quality and volume served as an argument for us to begin long-term spectroscopy to search for variability in the profiles of spectral features and the radial velocity pattern in time. This task requires repeated observations with high spectral resolution over a wide range of wavelengths. In this article, we present the results of the first stage of work. Section 2 of this article briefly describes the methods of observation and data analysis. Section 3 presents the results obtained, and sections 4 and 5 discuss the results in comparison with previously published ones, as well as summarize the main conclusions

## 2. ECHELLE SPECTROSCOPY AT BTA

Our first observations of CI Cam at the BTA were made using a moderate resolution spectrograph ( $R=12000$ ) PFES [16] on the night of December 3, 1998. This spectrum, containing only single-peaked emissions due to insufficient resolution, showed us the need and possibility of obtaining CI Cam spectra with a much higher resolution on the BTA. All subsequent CI Cam spectra were obtained by us at high resolution in 2002–2023 with echelle spectrograph NES [17], stationary located at the Nasmyth focus of the 6-m BTA telescope. The dates of observations are given in Table 1.

In recent years, the spectrograph has been equipped with a CCD detector with the number of elements  $4608 \times 2048$ , element size  $0.0135 \times 0.0135$  mm; readout noise  $1.8e^-$ . Wavelength range recorded in one exposure  $\Delta\lambda 470 \div 778$  nm. In 2001–2011 we used a CCD with a number of elements  $2048 \times 2048$ . To reduce flux losses at the entrance slit, the NES spectrograph is equipped with an imaha slicer. Using a slicer, each spectral order is repeated three times. The spectral resolution of the NES spectrograph  $R=\lambda/\Delta\lambda \geq 60\,000$ . In our CI Cam spectra, the signal-to-noise ratio ( $S/N$ ) varies by several orders of magnitude from the continuum to the peaks of strong emissions.

Extraction of one-dimensional data from two-dimensional echelle frames is performed using the ECHELLE context of the MIDAS package modified taking into account the geometry of the echelle frame. All details of the procedure are described in [18]. Traces of cosmic particles were removed using a standard technique – by median averaging a pair of spectra obtained sequentially. A Th–Ar lamp was used to calibrate the wavelengths. All subsequent steps in the processing of one-dimensional spectra were performed using the modern version of the DECH20t package [19]. Systematic error in heliocentric radial velocity measurements are based on a set of telluric features and interstellar lines of the Na I doublet, it does not exceed 0.25 km/s for one line; measurement error for broad absorptions does not exceed 0.5 km/s. For average velocity values in Table 1, errors are 0.6–2.4 km/s depending on the type of the measured lines. We identified features in the CI Cam

**Table 1:** Results of heliocentric radial velocity measurements in the spectra of CI Cam for different types of features. The number of details used in averaging the velocity is indicated in parentheses

Date	$\Delta\lambda$	Vr, km/s					
		JD	nm	Emis-d	Emis-s	[OIII]	DIBs
1	2	3	4	5	6		
04.02.2002	462–607	$-47.4 \pm 1.3$			$-51.2$	$-7.8$	
2452310.34		(43)				(2)	
19.11.2002	456–599	$-49.6 \pm 0.2$	$-47.4 \pm 0.8$	$-48.0$	$-7.4 \pm 0.7$		
2452598.16		(46)	(25)			(8)	
21.12.2002	452–599	$-51.7 \pm 0.2$	$-51.5 \pm 0.5$	$-55.2$			
2452630.44		(28)	(12)				
18.11.2005	528–670	$-53.8 \pm 0.2$	$-54.1 \pm 0.5$		$-7.8 \pm 0.7$		
2453693.40		(42)	(8)			(9)	
20.11.2005	528–670	$-54.6 \pm 0.4$	$-54.8 \pm 1.0$		$-6.0 \pm 0.5$		
2453694.51		(21)	(11)			(15)	
15.01.2006	456–601	$-54.4 \pm 0.2$	$-54.9 \pm 0.2$	$-51.6$			
2453751.20		(39)	(8)				
06.12.2006	447–593	$-55.1 \pm 0.2$	$-53.1 \pm 1.3$	$-54.7$	$-7.2 \pm 1.0$		
2454076.36		(61)	(14)			(6)	
07.12.2006	447–593	$-55.7 \pm 0.2$	$-53.3 \pm 0.4$	$-55.8$	$-7.8 \pm 0.9$		
2454077.22		(61)	(26)			(5)	
08.12.2006	447–593	$-55.6 \pm 0.2$	$-56.3 \pm 0.5$	$-54.8$	$-6.8 \pm 0.6$		
2454078.35		(59)	(19)			(7)	
10.12.2006	447–593	$-55.6 \pm 0.2$	$-56.2 \pm 0.5$	$-56.7$	$-7.0 \pm 1.0$		
2454080.35		(59)	(22)			(7)	
18.11.2008	447–593	$-55.6 \pm 0.2$	$-55.7 \pm 0.6$	$-56.3$			
2454788.29		(21)	(9)				
13.01.2011	520–668	$-54.0 \pm 0.2$	$-52.4 \pm 0.4$		$-6.6 \pm 0.7$		
2455575.26		(35)	(12)			(7)	
03.09.2015	395–698	$-54.4 \pm 0.2$	$-54.0 \pm 0.4$	$-55.1$	$-7.3 \pm 0.6$		
2457269.47		(88)	(35)			(17)	
08.12.2019	470–778	$-51.6 \pm 0.2$	$-51.9 \pm 0.7$	$-43.4$	$-7.6 \pm 0.3$		
2458826.45		(46)	(32)			(19)	
21.10.2021	470–778	$-51.5 \pm 0.3$	$-51.3 \pm 0.5$	$-43.0$	$-6.2 \pm 0.8$		
2459509.33		(49)	(23)			(17)	
05.07.2022	470–778	$-50.8 \pm 0.2$	$-50.0 \pm 0.2$	$-48.9$	$-6.2 \pm 0.5$		
2459890.37		(56)	(32)	(5)		(18)	
09.02.2023	470–778	$-51.1 \pm 0.3$	$-53.6 \pm 0.5$	$-48.4$	$-7.1 \pm 0.5$		
2459985.28		(60)	(12)			(10)	

spectra using lists of lines from papers based on spectroscopy at the BTA+NES of related stars with the B[e] phenomenon [20–22]. In addition, for several spectral details we used data from the VALD database (see [23] and references therein).

### 3. MAIN RESULTS

#### 3.1. Features of the CI Cam spectrum and their variability

The optical spectrum of CI Cam is populated by emissions of different types: emissions of metal ions with two-peaked “rectangular” profiles (hereafter – Emis-d), complicated not entirely symmetrical emissions of H I, He I, weak emissions of multiply ionized metals (Al III, Fe III, Si III, hereafter – Emis-s), emission components of the oxygen triplet OI 7773 Å. All of them are formed under different physical conditions in the circumstellar environment and have different widths. For this reason, we examined separately the time behavior of the profiles of these types of emissions and radial velocity from measurements of their positions.

In Figs. 1 and 2, these main features of the star’s spectrum are well illustrated. According to Beals classification [6], the H $\alpha$  profile belongs to type II – its single-peaked emission that does not contain absorption components. Figure 1 shows the H $\alpha$  profiles for several observational dates. The position of the dashed vertical line in this and subsequent figures corresponds to the accepted value  $V_{\text{sys}} = -55.4 \pm 0.6$  km/s for the [N II] line 5754 Å. Let us note the features detected in the H $\alpha$  profile: systematic decrease in the intensity of the profile top; lack of wind components; presence, in addition to a wide pedestal ( $\Delta V_r = \pm 400$  km/s), a slight increase in the intensity of the long-wavelength wing; its variability may be caused by the inhomogeneity of the circumstellar medium.

The profiles of double-peaked emissions (Fe II, [Fe II], etc.) have almost vertical slopes and concave peaks. In the case of a spherically symmetric and radially expanding wind, profiles with a flat top are formed in an optically thin medium. The observed shape of the vertices in the CI Cam spectrum indicates the structure of emitting layer. According to [3], the concavity of the profile, i.e., a decrease in emission, is due to less radiation at lower velocities. Even in the case of symmetry of the circumstellar medium, the tops of the profiles will not be flat even if there is additional absorption in the disk.

The variability of Fe II and [Fe II] emissions with “rectangular” profiles and concave peaks is illustrated in Fig. 3. This specific shape of Fe II and [Fe II] emissions persists during monitoring, however, the intensity of the emission peaks in the spectra obtained on different dates systematically changes. Noteworthy the right top panel, which shows a rarely observed ratio of peak intensities: the intensity of the long-wavelength peak for all emissions (except for the forbidden emission [N II] 5754 Å) is higher than the short-wavelength one.

On the left panel of Fig. 4, the profiles of the [N II] 5754 Å line in two early spectra of CI Cam (02/04/2002 and 11/19/2002) were compared with profiles obtained from 2008 to 2022. Here we see a significant difference between the early profiles of 2002 relative to all subsequent ones, which have the same the position of the short-wavelength wings and the intensity changes insignificantly. At the same time, in the earliest profile of 02/04/2002 we see an almost twofold increase in intensity, and a shift in position, a shift of the short-wave wing by about 10 km/s toward longer wavelengths. Already 8.5 months later, in November 2002, the intensity of this profile decreased significantly, and its short-wavelength wing approached the stationary position of the later profiles. The ratio  $V/R$  exceeds 1 for all observational epochs. The right panel of this figure shows the Fe II 5534 Å

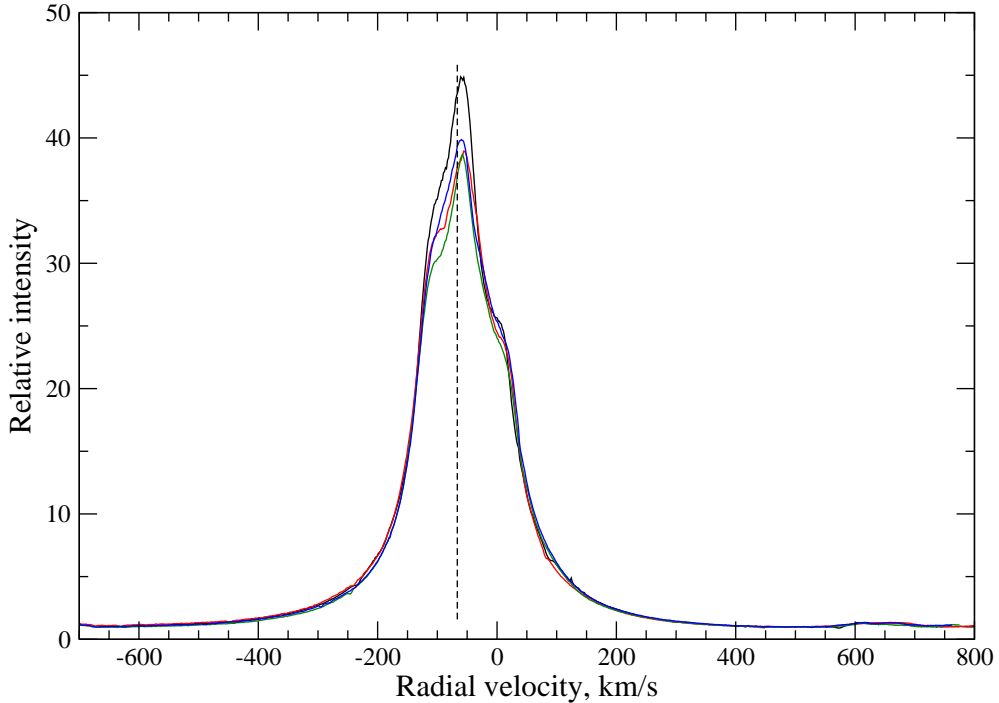


**Figure 1:** H $\alpha$  Profiles in CI Cam spectra obtained on different dates: November 18, 2005 (orange line), September 3, 2015 (black), October 21, 2021 (red), July 5, 2022 (green), February 9, 2023 (blue). Here and in subsequent figures, the position of the dashed vertical corresponds to the accepted value  $V_{\text{sys}} = -55.4 \pm 0.6$  km/s for the [N II] line 5754 Å, and the continuum level is taken as 1.

line profile for the same dates for comparison. For this line of low excitation in the spectra of 2002 we also see a shift of the short-wavelength wing by about 10 km/s red, but the behavior of the V/R value is different: the intensity changes insignificantly, in the spectra of 2002 the ratio  $V/R \geq 1$ , later  $V/R < 1$ .

Publications of the results of optical spectroscopy of CI Cam, as a rule, contain an indication of the presence of high excitation emissions in the spectra: He II 4686 Å, forbidden emissions [OI] 6300 and 6363 Å, [O III] 4959 and 5007 Å (see, for example, works [11, 12]). The [OI] 6300 and 6363 Å emission spectra are absent in our spectra, but the [O III] 4959 and 5007 Å lines are constantly observed. The identification of these weak lines of high excitation [O III] 4959 and 5007 Å does not cause problems, and the positions of both lines in the spectra,  $V_r(4959) = -52.4 \pm 1.6$  and  $V_r(5007) = -50.6 \pm 1.4$  km/s (averaged from 13 spectra), are in good agreement and change little over time.

The situation with the behavior of the He II 4686 Å emission in high-resolution spectra remains less certain. Eight of our spectra listed in Table 1 contain the wavelength range in which the presence of the 4686 Å line can be expected. In Fig. 5, fragments for 6 observational dates are presented. In spectra “1”, “3”, “4” and “5” this line is absent; in the spectrum “2” the emission intensity is low (about < 5% above the local continuum). In our earliest spectrum, obtained on December 3, 1998, with moderate resolution and  $S/N > 100$  with the PFES spectrograph, there is no emission at 4686 Å. And only in the spectrum, obtained on September 3, 2015, did a broad emission appear with an equivalent width of  $W_\lambda = 0.4$  Å. If we assume that this is the He II emission

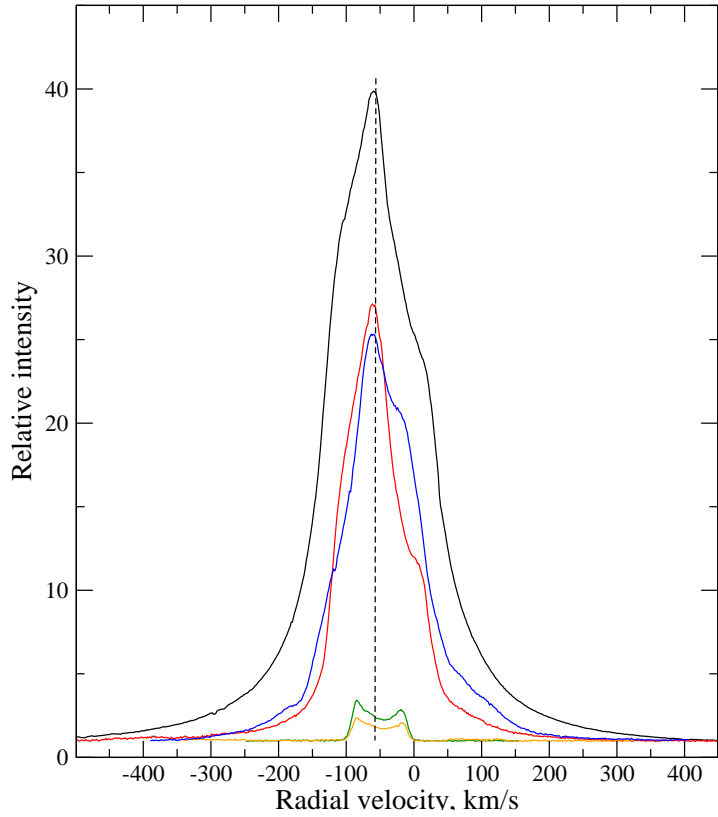


**Figure 2:** Profiles of specific emissions in the spectrum on February 9, 2023: H $\alpha$  (black line), H $\beta$  (red), HeI 5876 Å (blue), Fe II 5534 Å (green), Fe II 5425 Å (orange)

4686 Å, we obtain the width of its profile in the range of radial velocities from  $-100$  to  $+160$  km/s, which does not agree with the general picture of radial velocities in the system (see line profiles in Fig. 2) and raises the question of the localization of this emission in the CI Cam system.

The He II 4686 Å emission line may not appear in all orbital phases due, for example, to screening by dense regions of the shell of the main star of the system. In addition, it is weak and may not be visible against the background noise in spectra with low S/N ratios. Based on our observations, we can recognize the appearance of the He II 4686 Å emission in the spectra of CI Cam as a rare event, which indicates the difficulty of using this emission to estimate the period of the spectral variability of the star and raises the problem of localizing the emission in the CI Cam system. To solve this problem, there is an obvious need to obtain a significantly larger volume of high-quality spectral data. There is currently not enough high-resolution spectral data to support the use of this line for this purpose.

We also note that in the spectrum obtained on September 3, 2015, in which the emission was recorded near  $\lambda=4686$  Å, an additional feature is observed – a reduced intensity of emissions with “rectangular” profiles, which is well illustrated in the set of panels in Fig. 4.

### 3.2. Search for absorptions in CI Cam spectra

A close relative of CI Cam is the supergiant MWC 17 with the B[e] phenomenon, the features of which were studied in detail using several spectra of the BTA + NES by the authors [21]. The

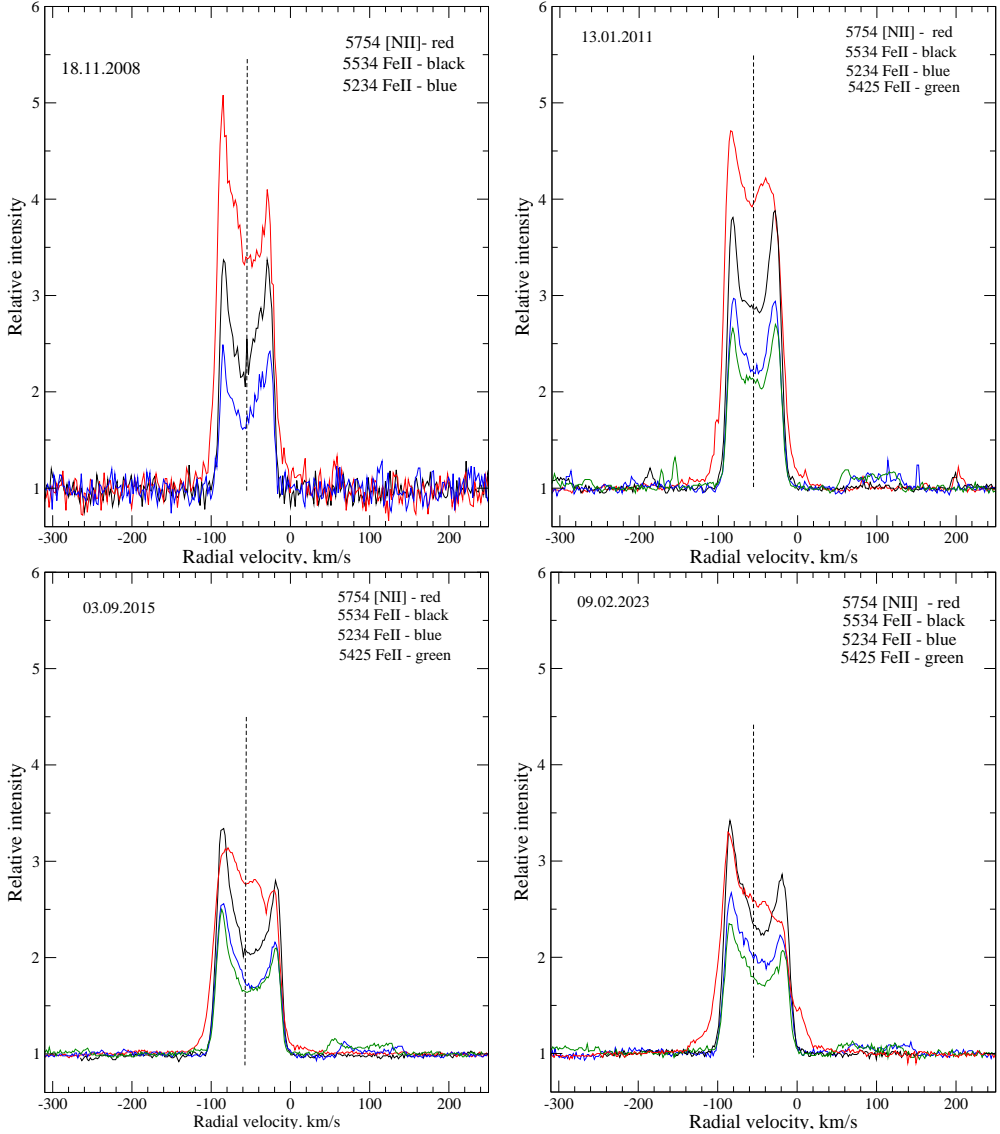


**Figure 3:** Profiles of selected lines in the spectra obtained on November 18, 2008, January 13, 2011, September 3, 2015, and February 9, 2023: [N II] 5754 Å (red line), Fe II 5534 Å (black), Fe II 5234 Å (blue), Fe II 5425 Å (green).

star MWC 17, identified with the IR source IRAS 01441+6026, is one of the hottest stars with the B[e] phenomenon. In its spectra taken in 2005–2006 numerous permitted and forbidden emissions, as well as interstellar Na I lines and diffuse interstellar bands (DIBs), have been identified. A comparison of the new data obtained with earlier measurements allowed us to conclude that there is no significant variability in spectral details. The pattern of radial velocities was studied using lines of various dates, which allowed the authors to accept the velocity of stable forbidden emissions as the systemic velocity,  $V_{\text{sys}} = -47$  km/s. The high quality of the spectral material used allowed the authors [21] perform detailed identification of spectral structures. A careful search did not lead to detection of absorptions formed in the stellar atmosphere in the spectrum of MWC 17. Having a sample of high-quality CICam spectra, we also undertook a search for similar absorptions, including a comparison of CICam spectra obtained on different dates. In the spectra of two

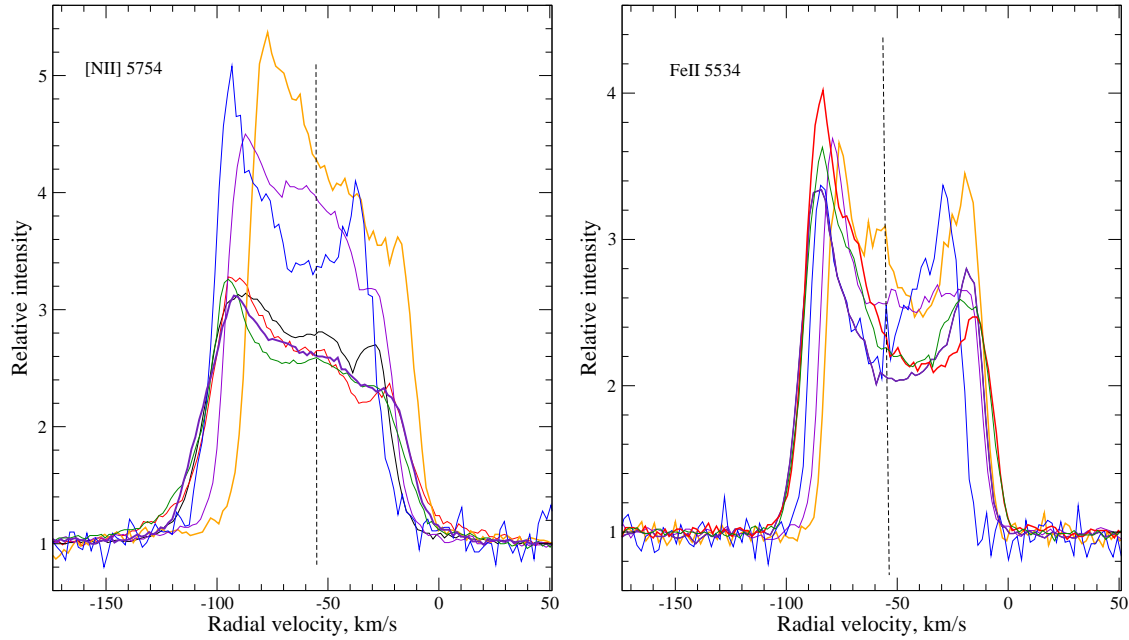


**Figure 4:** Emission profiles of [N II] 5754 Å (left) and Fe II 5534 Å (right) in spectra of different dates: February 4, 2002 (orange line), November 19, 2002 (purple), November 18, 2008 (blue), September 3, 2015 (black), December 8, 2019 (thick black line), October 21, 2021 (red), July 5, 2022 (green).

observatioaln dates in 2022 and 2023, we identified the absorptions of Fe III, N II and S II, and obtained average velocity with a good accuracy,  $V_r(\text{abs-2022}) = -32.4 \pm 0.5 \text{ km/s}$  (5 lines) and  $V_r(\text{abs-2023}) = -54.6 \pm 1.0 \text{ km/s}$  (9 lines), which gives rise to the conclusion about the presence of absorptions and the variability of their positions. In the spectrum obtained on December 8, 2019, we found only 5 absorptions; the average velocity for this date was determined with lower accuracy  $V_r(\text{abs-2019}) = -55.6 \pm 2.0 \text{ km/s}$ . The position of three of the found absorptions in two fragments of the spectra for three observational dates is shown in Fig. 6. From a comparison of fragments of the spectra of 2021, 2022 and 2023 we concluded on the absence of these absorptions in the spectrum of 2021. In general, we can talk about the presence of absorptions at certain moments of observations and the variability of their average position. Future spectral observations will serve to refine CI Cam's atmospheric spectrum information

### 3.3. CI Cam system velocity

The radial velocity corresponding to the position of the forbidden line [N II] 5754 Å is stable throughout all observation nights. The average velocity for this emission in 13 spectra was  $V_r(5754) = -55.4 \pm 0.6 \text{ km/s}$  and, as mentioned above, we accepted it as systemic, i.e.,  $V_{\text{sys}}(5754) = -55.4 \pm 0.6 \text{ km/s}$ . Two other forbidden [N II] lines with wavelengths 6548 and 6584 Å in the spectrum of CI Cam are located on the extended (up to 600 km/s) wings of powerful H $\alpha$  emission, and the second of them is also blended by closely spaced C II emissions, which somewhat reduces the measurement accuracy.

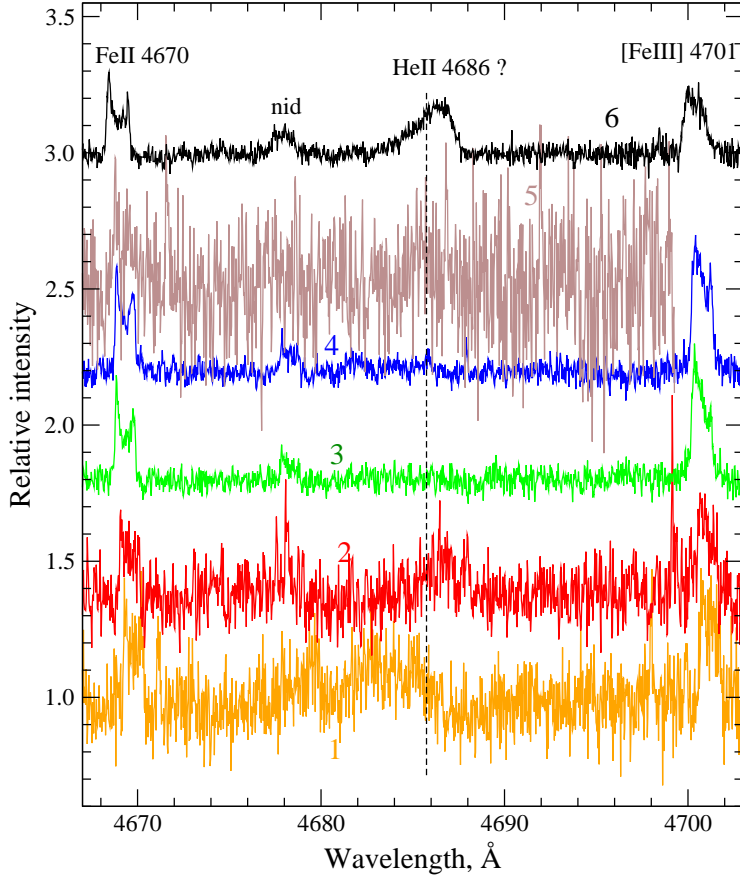


**Figure 5:** Fragments of CI Cam spectra in the wavelength range 4665–4703 Å, obtained on various dates: February 4, 2002 (orange line), January 15, 2006 (red), December 6, 2006 (green), December 7, 2006 (blue), November 18, 2008 (brown), September 3, 2015 (black line). The vertical position corresponds to a wavelength of 4686 Å. A weak emission at a wavelength around 4678 Å has not been identified.

#### 3.4. Comparison of the spectra of CI Cam and other stars with the B[e] phenomenon

From a comparison of the spectra of two B[e] supergiants, MWC 17 and CI Cam, it follows not only their fundamental similarity, but also differences in details. Let us emphasize the difference in the types of emission profiles: in the CI Cam spectra outside the outburst, the profiles of H $\alpha$ , H $\beta$ , Fe II, [Fe II], [O III] 5007 Å are single-peaked, but in the spectra of MWC 17 they are all double-peaked, which indicates a difference in the geometry and kinematics of the circumstellar medium. H $\alpha$  and [N II] lines in the spectra of both stars are shown in Fig. 7. In addition, the spectra of MWC 17 contain a number of emissions, [OI] 6300, 6363 Å, that are absent in the spectra of CI Cam. On the top panel of Fig. 8, fragments of the spectra of MWC 17 and CI Cam obtained with the NES spectrograph in December 2005 are compared. Both fragments contain the same lines, but their intensities differ significantly. The most powerful emission in this fragment, [OI] 6363 Å, prevails in the spectrum of MWC 17 and is completely absent in the spectral fragment of CI Cam. Of the forbidden oxygen emissions, only the [O I] 5577 Å emission is constantly present in all our CI Cam

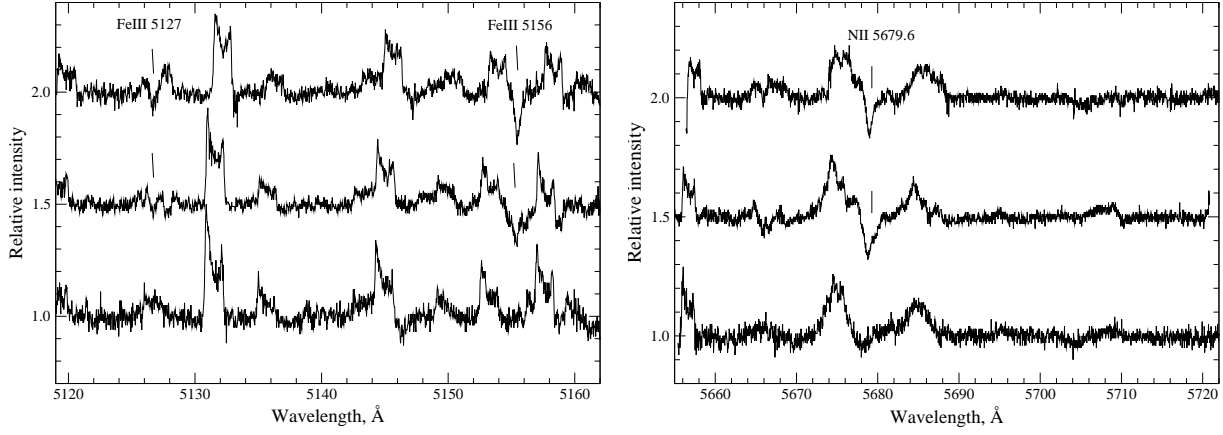


**Figure 6:** Fragments with absorptions in the CI Cam spectra, from top to bottom: February, 9, 2023, July 5, 2022, October 21, 2021. The two upper fragments are shifted along the ordinate axis by 0.5 and 1.0, respectively

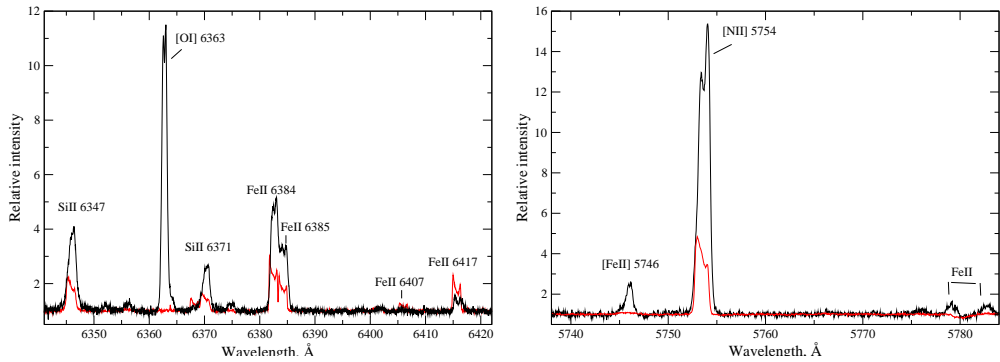


**Figure 7:** Comparison of fragments containing H $\alpha$  and forbidden lines [N II], in the spectra of MWC 17 (black line) and CI Cam (red), obtained on the BTA with the NES spectrograph in December 2005.

spectra, the profile width and position of which indicate telluric origin of this feature. M. Kraus [9] notes that forbidden [OI] emissions are formed in regions of the circumstellar medium with a low electron density.

Another emission feature was recorded in the CI Cam spectra – the OI 7773 Å triplet, which is shown in Fig. 9. An additionally plotted profile of the two-peaked Fe II 5432 Å emission from the same spectrum emphasizes the coincidence of the position of the short-wavelength wing of the left component of the triplet and the Fe II 5432 Å emission. The other two components of the triplet in the figure have a blend. The emission of the IR oxygen triplet is a peculiarity of the spectra of hot supergiants. In our studies of supergiants with gas-and-dust envelopes, we previously detected triplet emission in the spectra of the B[e] star in the system of the source IRAS 004770+6429 [24] and in the spectra of the B-supergiant LS III+52°24 (see [25], Fig. 6). This unstable post-AGB star, associated with the IR source IRAS 22023+5249, has a peculiar optical spectrum with a record high H $\alpha$  emission intensity and H $\beta$  with signs of winds of up to 290 km/s.

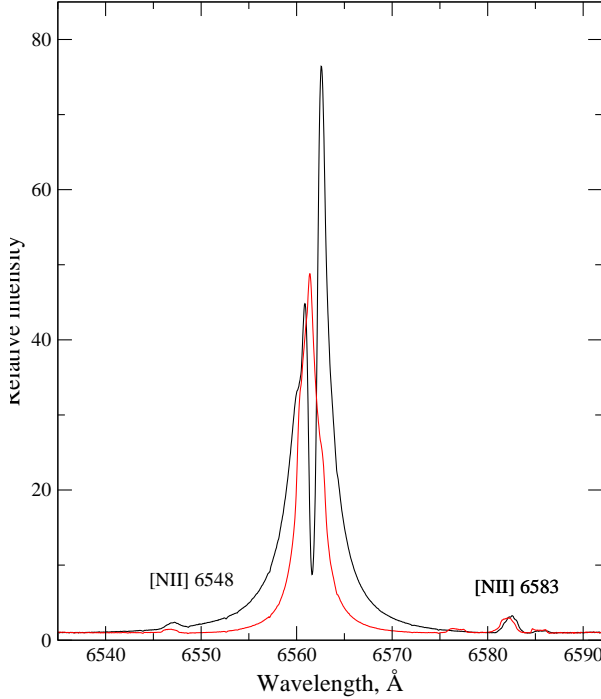


**Figure 8:** Comparison of fragments of the spectrum of MWC 17 (black line) and CI Cam (red), obtained on the BTA with the NES spectrograph in December 2005.

### 3.5. Interstellar details

The complex absorption-emission profiles of the NaI doublet remain virtually unchanged: measurements of the positions of their components in the available spectra allow the use of average values.

Average radial velocity for the permanently present components of NaI doublet lines:  $V_r(\text{NaI}) = -7.1 \pm 0.5$ ,  $-35.8 \pm 0.3$  and  $-77.7 \pm 0.8$  km/s, obtained by averaging measurements over 12 spectra. In Fig. 10, both multicomponents NaI D lines are shown in the spectrum obtained on October 2021. In addition to the main components (circumstellar emission “1” and interstellar absorptions “2”, “3”), these profiles also contain a telluric emission “4”. The dashed vertical lines in the figure indicate the average position of the two interstellar components ( $V_r(\text{KI}) = -7.0$  and  $-36.7$  km/s) of the line KI 7696 Å. The average velocity  $V_r(\text{DIBs})$  in 11 spectra,  $V_r(\text{DIBs}) = -7.04 \pm 0.21$  km/s, coincides with the velocity of the long-wave components of the NaI and KI lines profiles. Systemic velocity of CI Cam  $V(\text{LSR}) \approx 50$  km/s and the presence of short-wave interstellar absorption in the spectrum indicate a significant distance of CI Cam in the Perseus arm, according to the velocity pattern in the Galaxy [26], which is consistent with the parallax of the star  $\pi = 0.2101$  mas from the Gaia DR3 catalog.

By measuring the equivalent widths of the DIBs in the spectra and using calibrations [27], we appreciated the excess color (see Table 2). Its average value over 9 DIBs bands  $E(B - V) = 0.74 \pm 0.06^m$ . Using the standard ratio value  $A_v/E(B - V) = 3.2$ , we obtain an estimate of an interstellar extinction  $A_v = 2.4^m$ . Authors [8], by analyzing absorption estimates obtained from SED modeling, indicate total extinction values  $A_v = 3.71^m$  and higher, up to  $4^m$ , which leads to

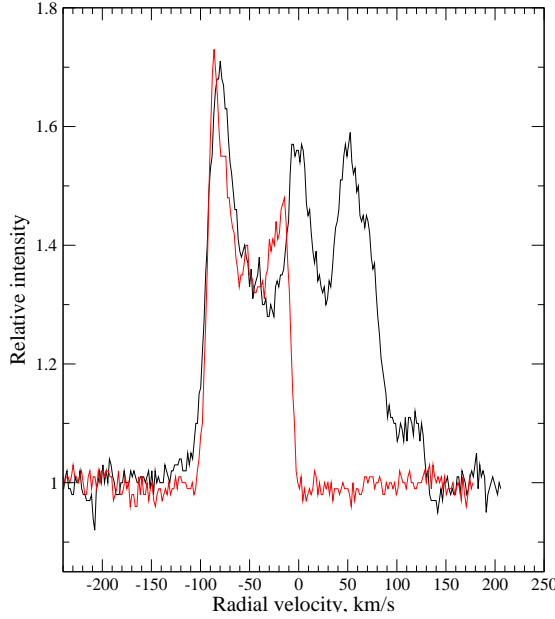


**Figure 9:** Oxygen triplet O I 7773 Å (black line) in the CI Cam, spectrum obtained on July 5, 2022. The red line is the profile of the two-peaked emission of Fe II 5432 Å in the same spectrum.

**Table 2:** Table 2. Equivalent widths  $W_\lambda$ (DIBs) averaged over CI Cam spectra. The last column shows the corresponding color excess values  $E(B - V)$  using calibrations [27].

$\lambda$ , Å	$W_\lambda$ (DIBs), mÅ	$E(B - V)$ , mag
5705.20	54±4	0.5
5780.48	376±14	0.7
5797.06	126±12	0.8
5849.81	38±6	0.5
6195.98	51±4	0.85
6203.05	121±20	1.0
6379.32	76±5	0.65
6613.62	188±3	0.75
6660.71	51±4	0.9

greater distance CI Cam,  $d > 4$  kpc.

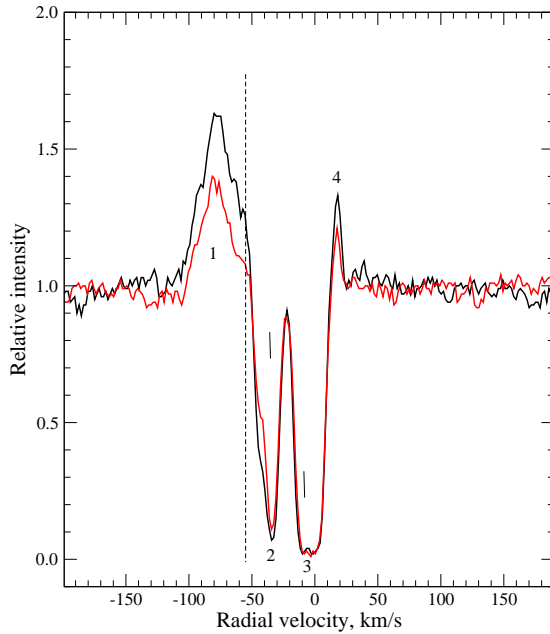


**Figure 10:** Line profiles of NaI 5889 Å (black line) and NaI 5895 Å (red) in the CI Cam spectrum obtained on October 21, 2021. Short vertical lines indicate the average position of the two interstellar components,  $V_r(KI) = -7.0$  km/s and  $-36.7$  km/s, line K I 7696 Å

#### 4. DISCUSSION OF RESULTS

The group of [Be] stars is heterogeneous, this is well illustrated by the features of the observed emission profiles in [28] as well examples of model profiles of specific lines [7]. The optical spectra of CI Cam contain double-peaked and single-peaked emissions from metals as well as single-peaked emissions from the H I and He I lines. From the list of main line categories [7], typical for the spectra of stars with the B[e] phenomenon, there are no normal profiles of the P Cyg type. At present, it is necessary to confirm the presence of absorptions arising in the stellar atmosphere, which we found in the spectra of 2022. Among the forbidden lines, those of low-excitation ions, formed in the outer zone of low density, dominate. High excitation lines like [S III] are rarely observed. In particular, this emission is absent from our CI Cam spectra. However, a pair of single-peaked high-excitation [O III] emissions at 4959 and 5007 Å is constantly present. Their intensity is low, only 2–3% above the level of the local continuum, however, their position is stable and the average radial velocity for these forbidden emissions for each date, indicated in the 5-th column of the Table 1 is no different from the general picture of velocities.

It is also necessary to mention on the features of the He II 4686 Å emission, whose behaviour was used [29, 30] to study radial velocity variability in the system and determine the orbital period. Using data obtained from various moderate and high resolution spectrographs, these authors identified a high amplitude (up to 500 km/s) velocity variability and determined an orbital period of about 19 days. However, having a homogeneous sample of spectra, we cannot confirm this result and can only talk about the rare appearance of emission near the wavelength 4686 Å. Observational data from other authors also do not allow us to identify this feature with the high excitation line of He II 4686 Å. Bartlett et al. [3], having obtained two high-resolution spectra in October 2016, also did not find the presence of the He II 4686 Å feature and highlighted the

unreliability of using this line to determine the orbital period. Let us also recall the results of the paper [28], the authors of which, citing characteristic emissions for a sample of B[e] stars, emphasize the absence in the spectrum of CI Cam of the most typical emissions for objects of this type: [Ca II] 7291 and 7324 Å, as well as [O I] 6300 and 6363 Å. In a later publication [31] the absence of He II 4686 Å emission was also noted.

We have already mentioned above the object MWC 17, which has similar features of the optical spectrum. As shown based on direct H $\alpha$  images authors [32], both stars, MWC 17 and CI Cam, stand out in the sample of stars with the B[e] phenomenon in the absence of extended H $\alpha$ -shells. On the other hand, the combination of a number of observed features in the spectrum of CI Cam makes this object similar to another supergiant MWC 137. Long-term study allows us to finally classify MWC 137 as a supergiant with the B[e] phenomenon (see details and links in [33]). In addition to its peculiar optical spectrum, this object is also interesting because it is a member of a stellar group and is surrounded by an extended H $\alpha$  Sh2-266 nebula. In the context of our paper, the B[e] supergiant MWC 137 is useful for comparing its properties with those of CI Cam. In the optical spectrum of MWC 137 the profile H $\alpha$  has similar features to CI Cam, except for its extreme width; Fe II emissions are double-peaked; as in the spectrum of CI Cam. The spectra of MWC 137 lack the typical disk emissions [O I] 5577 Å, [Ca II] 7291 and 7324 Å, as well as photospheric absorptions. This similarity in the details of the optical spectrum allows us to classify CI Cam as a B[e] supergiant

Analysis of the set of radial velocity measurements allows us to speak about the stability of the kinematic state in the CI Cam system. Based on measurements of the radial velocity from the positions of numerous “rectangular” emissions in the spectra of the star, a weak variability of the radial velocity was found in the interval  $V_r(\text{emis-d}) = -50.8 \div -55.7 \pm 0.2$  km/s. The radial velocity corresponding to the position of the forbidden line [N II] 5754 Å is stable throughout all observations,  $V_r = -55.4 \pm 0.6$  km/s, and we accepted it as systemic. Moreover, a comparison of the profiles of numerous “rectangular” emissions, including [N II] 5754 Å in the spectra of various nights after the 1998 outburst, indicates a systematic change in the intensity of the profile peaks.

## 5. CONCLUSIONS

Below we list our main results and conclusions:

- for all dates of CI Cam observations, “rectangular” profiles of two-peaked forbidden and permitted emissions of metal ions were recorded. The intensities of their blue-shifted peaks are higher than red-shifted peaks for all observational dates, with the exception of the spectrum of January 13, 2011 with an inverse V/R ratio and the spectrum of November 18, 2008 with equal peak intensities;
- a significant decrease in the intensities of all emissions with “rectangular” profiles was found with increasing distance in time from the 1998 outburst;
- the H $\alpha$  is not completely symmetric and contains additional variable parts. At a constant position of the line profile as a whole, changes in the intensity of the profile top and additional details are observed;
- the kinematic state of the CI Cam system is stable, average emission velocity for all observational dates  $V_r(\text{aver}) = -53.1 \pm 0.5$  km/s. The half-amplitude of the variations (root mean square deviation) is  $\Delta V_r = 2.5$  km/s;

- the behavior of the forbidden line [N II] 5754 Å does not differ from those of other emissions: the radial velocity corresponding to its position is stable in our observations after 2002 and is accepted by us as systemic,  $V_r = -55.4 \pm 0.6$  km/s;
- a rarely observed emission feature was discovered in the spectra of CI Cam — the emissive nature of the components of the O I 7773 Å triplet;
- the conclusion about the absence of emissions of [O I] 6300 and 6363 Å, [Ca II] 7291 and 7324 Å was confirmed. The intensity and position of the emission near 4686 Å vary significantly. The significant intensity of this line, about 16% of the local continuum, was recorded only in the spectrum obtained in September 2015. The currently available high-resolution spectra do not make it possible to resolve the issue of the reliability of this feature for estimating the orbital period of the star and the localization of this emission in the CI Cam system. The need to increase the volume of high-quality spectra is obvious;
- by measuring the equivalent widths of the DIBs and using published calibrations, we estimated the color excess  $E(B-V)$  due to interstellar extinction. Its average value over 9 DIBs bands is  $E(B-V) = 0.74 \pm 0.06$ . Using the standard ratio  $A_v/E(B-V) = 3.2$  we obtain an estimate of interstellar extinction  $A_v = 2.4 \pm 0.2$ ;
- in the spectra of 2022 and 2023, photospheric absorptions of Fe III, N II, Ti II and S II were identified, which made it possible to obtain average radial velocity with a good accuracy,  $V_r(\text{abs-2022}) = -32.4 \pm 0.5$  km/s (5 lines) and  $V_r(\text{abs-2023}) = -54.64 \pm 1.0$  km/s (9 lines), and gives grounds for the conclusion about the presence of absorptions and the variability of their positions. In the spectrum of December 8, 2019, we also found 5 absorptions; the average velocity for this date was determined with lower accuracy,  $V_r(\text{Vr-2019}) = 55.6 \pm 2.0$  km/s. The 2021 spectrum contains only two N II absorptions.

In general, we can talk about the stability of the kinematic picture of the CI Cam system in a sleeping state; we have not recorded any dramatic changes over the course of 20 years. But, at the same time, the CI Cam spectra exhibit essential variability in the intensity of emissions of all types, which may be a manifestation of the inhomogeneity of physical conditions in the circumstellar envelope. We consider an important result of the work to be the discovery for a number of observational moments of photospheric-type absorptions with variability of their average position. This result also requires the accumulation of high-resolution spectral data. It is clear that the CI Cam system needs continued observation and a deeper study.

## FUNDING

Observations with the 6-meter telescope of the Special Astrophysical Observatory of the Russian Academy of Sciences were supported by the Ministry of Science and Higher Education of the Russian Federation.

We thank the Russian Science Foundation for financial support (grant no. 22-12-00069).

The work used information from the astronomical databases SIMBAD, VALD, SAO/NASA ADS, and Gaia DR3.

## CONFLICT OF INTERESTS

The authors of this work declare that they have no conflicts of interest.

## REFERENCES

1. P.W. Merrill, C.G. Burwell. *Astrophys. J.*, **78**, 87 (1933).
2. J.S. Clark, A.S. Miroshnichenko, V.M. Larionov, V.M. Lyuty, R.I. Hynes, G.G. Pooley, M.J. Coe, M. McCollough, S. Dieters, Yu.S. Efimov, J. Fabregat, V.P. Goranskii, C.A. Haswell, N.V. Metlova, E.L. Robinson, P. Roche, P.I. Shenavrin, W.F. Welsh. *Astron & Astrophys.*, **356**, 50 (2000).
3. E.S. Bartlett, J.S. Clark, I. Negueruela. *Astron & Astrophys.*, **622**, A93 (2019).
4. H.J.G.L.M. Lamers, F.-J. Zickgraf, D. de Winter, L. Houziaux, J. Zorec. *Astron & Astrophys.*, **340**, 117 (1998).
5. A.S. Miroshnichenko, V.G. Klochkova, K.S. Bjorkman, V.E. Panchuk. *Astron & Astrophys.*, **390**, 627 (2002).
6. G.S. Beals. *MNRAS*, **91**, 966 (1931).
7. F.-J. Zickgraf. *Astron & Astrophys.*, **408**, 257 (2003).
8. R.I. Hynes, J.S. Clark, E.A. Barsukova, P.J. Callanan, P.A. Charles, A. Collier Cameron, S.N. Fabrika, M.R. Garcia, C.A. Haswell, Keith Horne, A. Miroshnichenko, I. Negueruela, P. Reig, W.F. Welsh, and D.K. Witherick. *Astron & Astrophys.*, **392**, 991 (2002).
9. M. Kraus. *Galaxies*, **7**, (4) id 83 (2019).
10. G. Maravelias, M. Kraus, L.S. Cidale, M. Borges Fernandes, M.L. Arias, M. Cure, G. Vasilopoulos. *MNRAS*, **480**, 320 (2018).
11. E.L. Robinson, I.I. Ivans, W.F. Welsh. *Astrophys. J.*, **565**, 1169 (2002)
12. J. Yan, Q. Liu, H. Hang. *Astron. J.*, **133**, (4) 1478 (2007).
13. N.D. Thureau, J.D. Monnier, W.A. Traub, R. Millan-Gabet, E. Pedretti, J.-P. Berger, M.R. Garcia, F.P. Schloerb, A.-K. Tannirkulam. *MNRAS*, **398**, 1309 (2009),
14. V.P. Goranskij, E.A. Barsukova, K.S. Bjorkman, A.N. Burenkov, V.G. Klochkova, N. Manset, N.V. Metlova, A.S. Miroshnichenko, V.E. Panchuk, M.V. Yushkin, S.V. Zharikov. In: “The B[e] Phenomenon: Forty Years of Studies”, Proceedings of a Conf. held at Charles University, Prague, Czech Republic 27 June–1 July 2016. Eds by A. Miroshnichenko, S. Zharikov, D. Korčaková and Marek Wolf. *ASP Conf. Series*, **508**. San Francisco: Astronomical Society of the Pacific, p.307 (2017).
15. C.S. Kochanek, B.J. Shappee, K.Z. Stanek, T. W.-S. Holoiien, Todd A. Thompson, J.L. Prieto, Subo Dong, J.V. Shields, D. Will, C. Britt, D. Perzanowski, G. Pojmański. *PASP*, **129**, 104502 (2017).
16. V.E. Panchuk, I.D. Najdenov, V.G. Klochkova, A.B. Ivanchik, S.V. Yermakov, V.A. Murzin. *Bull. Special Astrophys. Obs.*, **44**, 127 (1997)
17. V.E. Panchuk, V.G. Klochkova, M.V. Yushkin. *Astronomy Reports*, **61**, (9) 820 (2017).
18. M.V. Yushkin and V.G. Klochkova. *Special Astrophysical Observatory*, Preprint No. 206, (2005).
19. G.A. Galazutdinov. *Astrophys. Bull.*, **77**, (4) 519 (2022).
20. A. Aret, M. Kraus, M. Šlechta. *MNRAS*, **456**, 1424 (2016)
21. A.P. Marston, B. McCollum. *Astron & Astrophys.*, **477**, 193 (2008).

22. E.L. Chentsov, V.G. Klochkova, A.S. Miroshnichenko. *Astrophys. Bull.*, **65**, (2) 150 (2010).
23. V.G. Klochkova, E.L. Chentsov. *Astrophys. Bull.*, **71**, (1) 33 (2016).
24. A.S. Miroshnichenko, V.G. Klochkova, E.L. Chentsov, V.E. Panchuk, M.V. Yushkin. N. Manset. *MNRAS*, **507**, 879 (2021).
25. F. Kupka, N. Piskunov, T.A. Raybchikova, H.C. Stempels, W.W. Weiss. *Astron & Astrophys. Suppl. Ser.*, **138**, 119 (1999).
26. A.S. Miroshnichenko, E.L. Chentsov, V.G. Klochkova, S.V. Zharkov, K. N. Grankin, A.V. Kusakin, T.L. Gendet, G. Klingenberg, S. Kildahl, R.J. Rudy, D.K. Lynch, C.C. Venturini, S. Mazuk, R.C. Puetter, R.B. Perry, A.C. Carciofi, K.S. Bjorkman, R.O. Gray, S. Bernabej, V.F. Polcaro, R.F. Viotti, L. Norci. *Astrophys. J.*, **700**, 209 (2009).
27. V.G. Klochkova, A.S. Miroshnichenko, V.E. Panchuk, N.S. Tavolzhanskaya, M.V. Yushkin. *Astronomy Reports*, **66**, (5) 429 (2022).
28. J.P. Vallée. *Astron. J.*, **135**, (4) 1301 (2008).
29. J. Kos & T. Zwitter. *Astrophys. J.*, **774**, 72 (2013).
30. E.A. Barsukova, N.V. Borisov, A.N. Burenkov, V.P. Goranskii, V.G. Klochkova, N.V. Metlova. *Astronomy Reports*, **50**, (8) 664 (2006).
31. E.A. Barsukova, A.N. Burenkov, V.P. Goranskij, S.V. Zharkov, L. Iliev, N. Manset, N.V. Metlova, A.S. Miroshnichenko, A.V. Moiseeva, P.L. Nedialkov, E. Semenko, K. Stoyanov, I. Yakunin. *Astrophys. Bull.*, **78**, (1) 1 (2023).
32. A. Aret, M.L. Arias, A. Torres, L.S. Cidale, T. Eenmäe. *BAAS*, **61B**, (2020).
33. M. Kraus, T. Liimets, C.E. Cappa, L.S. Cidale, D.H. Nickeler, N.U. Duronea, M.L. Arias, D.S. Gunawan, M.E. Oksala, M. Borges Fernandes, G. Maravelias, M. Cure, M. Santander-Garcia. *Astron. J.*, **154**, (5) 186 (2017).